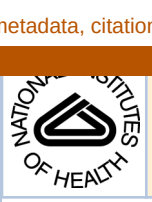

Published in final edited form as:

Brain Res Bull. 2010 May 31; 82(3-4): 169–176. doi:10.1016/j.brainresbull.2010.04.001.

Dysfunction of the magnocellular stream in Alzheimer's disease evaluated by pattern electroretinograms and visual evoked potentials

F. Sartucci[a,b,*], **D. Borghetti**[a], **T. Bocci**[a,c], **L. Murri**[a], **P. Orsini**[d], **V. Porciatti**[e], **N. Origlia**[b], and **L. Domenici**[f,b]

[a]Department of Neuroscience, Unit of Neurology, Pisa University Medical School, Pisa, Italy

[b]Institute of Neuroscience, National Research Council, Pisa, Italy

[c]Department of Neurological Neurosurgical and Behavioural Sciences, Siena University Medical School, Siena, Italy

[d]Department of Biochemical Sciences and Physiology and Biochemistry, Pisa University Medical School, Pisa, Italy

[e]Bascom Palmer Eye Institute, Miami, FL, USA

[f]Department of Biomedical Sciences and Technology, School of Medicine, University of L'Aquila, L'Aquila, Italy

Abstract

Background—Visuo-spatial disturbances could represent a clinical feature of early stage Alzheimer's disease (AD). The magnocellular (M) pathway has anatomo-physiological characteristic which make it more suitable for detecting form, motion and depth compared with parvocellular one (P).

Objective—Aim of our study was to evaluate specific visual subsystem involvement in a group of AD patients, recording isoluminant chromatic and luminance pattern electroretinograms and pattern visual evoked potentials.

Material and methods—data were obtained from 15 AD patients (9 females and 6 males, mean age ± 1SD: 77.6 ± 4.01 years) not yet undergoing any treatment, and from 10 age-matched healthy controls. Diagnosis of probable AD was clinically and neuroradiologically established. PERGs were recorded monocularly in response to equiluminant red-green (R-G), blue-yellow (B-Y) and luminance yellow-black (Y-Bk) horizontal square gratings of 0.3 c/deg and 90% contrast, reversed at 1 Hz. VEPs were recorded in response to full-field (14 deg) equiluminant chromatic R-G, B-Y and luminance Y-Bk sinusoidal gratings of 2 c/deg, presented in onset (300 ms)–offset (700 ms) mode, at the contrast levels of 90%.

Results—All data were retrieved in terms of peak-amplitude and latency and assessed using the Student's *t*-test for paired data. Temporal differences of PERGs and VEPs, evoked by Y-Bk grating in AD patients compared with controls, suggest a specific impairment of the magnocellular stream.

[*]Corresponding author at: Neurology, Pisa University Medical School, Neuro-science Department, Unit of Outpatient Neurology, Via Paradisa, n. 2, I 56124 Pisa, Italy. Tel.: +39 050 996760/996767; fax: +39 050 550563/996767. f.sartucci@neuro.med.unipi.it (F. Sartucci). URL: http://www.unipi.it (F. Sartucci).

Conflict of interest

We disclose any actual or potential conflict of interest including any financial, personal or other relationships with other people or organizations within three years of beginning our work submitted that could inappropriately influence it.

Conclusions—Our study support the hypothesis that the impairment of the PERGs and VEPs arising from the magnocellular streams of visual processing may indicate a primary dysfunction of the M-pathways in AD.

Keywords

Chromatic stimuli; Pattern electroretinograms; Pattern visual evoked potentials; Magno-; parvo-; konio-cellular subsystem; Alzheimer's disease

1. Introduction

Alzheimer's disease (AD) is a chronic neurodegenerative disorder of elderly characterized by specific pathological changes resulting in progressive development of cognitive impairment leading to dementia [40]. A plethora of different theories and hypothesis have been put forward to explain the pathogenesis and development of the disease. However, the cause of the sporadic form of the disease is unknown, probably because it is pleiotropic, caused by ageing in concert with a complex interaction of both genetic and environmental risk factors [19,26,87].

Histopathological studies have demonstrated that hippocampus and the parahippocampal regions are the earliest affected regions during AD, suggesting a precise chronological (and hierarchical) order of involvement: from limbic to associative cortical areas, from associative to primary sensory cortical areas including the visual cortex. Following this scheme, the involvement of visual system characterizes a late phase of AD [23,58]. However, recent studies have highlighted an apparent dichotomy between the progress of histopathological findings in different brain areas and the occurrence of visual dysfunctions in AD animal model and patients. For example, a recent report has shown that soluble beta-amyloid affects different types of circuitry in mouse primary visual cortex supporting the idea that visual system might be functionally impaired even at an early stage of AD [55]. In addition, clinical studies support a link between cognitive performance and visual dysfunction even at an early stage of AD. Indeed, the gradual loss of memory and attention are frequently accompanied by alteration of visuo-spatial function in animal models and AD patients [31,70]. Undoubtedly, sensory troubles including visual deficits add to and perhaps exacerbate learning/memory alterations characterizing AD. Among the clinical signs of AD, visual impairments ranging from visuo-spatial deficits, topographic agnosia, visual agnosia and Balint's Syndrome have been described [8,30,45]. In addition, several authors have reported a reduction of visual acuity in AD [12,37], as well as an abnormal contrast sensitivity, mainly at lowest frequencies tested [14,61], and colour discrimination deficits, especially for blue hues [13].

However, visual impairment such as visuo-spatial, colour and motion perception deficits can be difficult to evaluate in patients with normal routine eye evaluation without the use of specific psychophysics and electrophysiologic exams [39,44,52,54,73,75,77,86]. Thus, it turns to be important the issue on how to evaluate subtle and specific deficits affecting different visual subsystems in AD patients.

The post-receptorial visual pathways of primates contain two major parallel streams specific for colour contrast/form discrimination and luminance contrast/movement discrimination, respectively [17,20,38,41,47,68,79,80,82]. The colour-opponent system originates from small, tonic ganglion cells relaying to parvocellular laminae of the lateral geniculate nucleus and then projecting to layer 4C-β of the striate cortex. More deeply, recent data showed that two colour-opponent pathways, red-green (R-G) and blue-yellow (B-Y), form the so-called parvo- (P) and konio-cellular (K) streams, respectively [16,38,41,43,48,59,60]. The second

major subsystem, i.e. the achromatic stream, originates from large, phasic ganglion cells projecting to the magnocellular (M) layers of the lateral geniculate nucleus and then to laminae 4C-α of the striate visual cortex [16,21,38,41,43,48,59,60]. It is worth to note that parvocellular cells may also respond well to achromatic contrast stimuli of relatively high-spatial frequency. However, within the range of spatial frequencies to which both streams respond, M cells are relatively more sensitive to achromatic contrast and this characteristic is more prominent at higher temporal frequencies. To date, it is common knowledge that a specific decline in high-spatial contrast and low-temporal frequency sensitivity suggests a selective deficit in P-stream [18,35], whereas the loss of motion perception and the impairment in analyzing low-spatial frequency and contrast luminance are more likely to be related with severe dysfunction affecting M-pathway [23]. Impairments in motion perception and target tracing are considered to be a relatively common, however not selective, symptoms after dementia onset in AD [13]. Specific involvement of the magno-cellular stream of visual processing is particularly important since cell loss, prevalent deposition of amyloid plaques and neurofibrillary tangles occur in the primary visual cortex of AD individuals with a prevalence in the M-pathway [38,39]. Our findings are consistent with the supposition that AD determines primary sensory disruption. In the past, the reason for a caution interpretation of previously reported evidences is that there are many contradictory signs of a specific visual involvement: shrinkage of both P and M ganglion cells in the retina [23], thinning of the nerve fiber layer [5], as well as pathology in both the magno- and the parvocellular layers of lateral geniculate nucleus (LGN) [31], without any definitive conclusion on the selective vulnerability of a visual subsystem.

The present paper proposes the use of electrophysiological exams able to unveil visual dysfunctions of different visual streams in AD patients. Electrophysiological recordings of electroretinograms (ERGs) and visual evoked potentials (VEPs) have been already applied in AD patients. For example in demented patients, the late components (N130, P165, N220) of the VEPs are often delayed [84,85], even though the waveform shapes do not substantially change over the adult span [67]. However their relationship with either P- or M-pathways damage remains uncertain.

Results from several studies have shown that the magnocellular dominated layers 4C-α and 4B and send axonal direct projections to the superficial layers within primary visual cortex [2,25].

Although recent studies suggest that segregation between main visual streams is not complete [83], the present paper addresses the hypothesis that AD involves a deficit in the magnocellular pathway of the visual system using ERGs and VEPs to chromatic (Ch) and luminance (Lum) stimuli.

Besides that, electrophysiological analysis of these three different streams might be relatively simple also considering that sensory inputs are conveyed to the LGN, and then to V1 cortical area, in a one-to-one ordered fashion. Previous reports showed that luminance and chromatic contrast sensitivity develop independently at different rates, probably reflecting a different development of postreceptoral neural mechanisms [9,23].

Perhaps, using sinusoidal gratings, there is no need to assess individual visual acuity, neither to correct any refractory deficit, optical aniseikonia or study AD patients separately in terms of time of disease onset, educational level, disease duration and presence or predominance of specific behavioral symptoms. Sinusoidal grating patterns in fact elicit responses that are minimally or not influenced by small refractive deficit, if not adequately corrected, and represent the best stimuli for both electrophysiology and spatial contrast sensitivity tests [10,59].

We raise the hypothesis that AD involves a deficit in the M-pathway resulting in subtle dysfunction at the level of retina, post-retinal pathways and/or visual cortex. To this aim we recorded electroretinograms and visual potentials evoked by chromatic and luminance visual stimuli (ChPERGs and ChVEPs, Lum ERGs and LumVEPs) in a selected sample of AD patients and compared results with a control group of age and sex matched healthy subjects.

2. Patients and methods

2.1. Patients and controls

The study was conducted on 15 recently diagnosed patients defined as probable AD, selected from cases referred to our Neurodegenerative Diseases Centre, nine of them were females and six males (mean age ± SD: 77.6 ± 4.01 years; range 72–86); they all have been diagnosed for the first time in the month preceding the inclusion in the study. AD patients met the diagnostic criteria of probable AD according to the Diagnostic and Statistical Manual of Mental Disorders, fourth edition (DSM-4), the ICD-10 Classification of Mental and Behavioral Disorders (ICD-10) and the criteria of the National Institute of Neurologic and Communicative Disorders and Stroke and the Alzheimer's Disease and Related Disorders Association (NINCDS-ADRDA [44]). Severity of dementia was assessed using MMSE [15], even if patients have been examined by means of a extensive standardized diagnostic protocol [78]; at the time of diagnosis, all the patients. presented a MMSE score below 23/30. Diagnosis of AD was supported by a exhaustive diagnostic work-up including morphological and functional neuroimaging. In particular each patient underwent a brain MRI scan and a FDG-PET semi-quantitative study, electroencephalogram and auditory P300 Event Related Potentials (ERPs). Other possible causes of dementia were excluded. The disease onset was homogeneous among patients and disease duration from onset varied from 12 to 16 months; no one case showed a cerebrovascular load more than two minor lacunar microlesions, as proved by neuroimaging. Moreover, we considered as normal small areas of long T2 MRI-imaging around the frontal horns, reflecting either mild and age-related white matter changes or minor ischemic events [22,90]. In addition, infarcts and white matter low attenuation (WMLA) on CT were assumed to be of differential diagnostic value between vascular and degenerative dementia [34]. Inclusion criteria are summarized in Table 1.

Ten healthy volunteers, five males and five females (age range 69–84 years; mean age ± SD: 75.3 ± 6.2 years), were enrolled as a control group; control group was made of subject *ad hoc* selected among people of the department staff and relatives or friends of investigators, age, sex and education levels were analogous with those of patients; they had never prior used in other experiments.

All subjects (patients. and controls) underwent a extensive clinical neuro-ophthalmological examination, including Snellen visual acuity testing (monocular), pupillary function evaluation, fundoscopic and chromatic vision. No patient had involuntary eye movement or spontaneous nystagmus, neither ophthalmologic disease, including mild cataract, incipient macular degeneration, and congenital colour anomaly (Ishihara).

None of the patients was intaking medications, or any psychotropic drugs (sedatives, neuroleptics or antiepileptics) at the time of inclusion in the study or at least 1 month before and they all had suspended alcohol consumption at least 48 h before exams. All had a visual acuity of ≥0.8 Snellen fraction or better (mean visual acuity: 9.0 ± 0.6); the diameter of undilated pupils was 4–5 mm in both control subjects and patients. We also excluded patients with suspected psychiatric disorders that might complicate the assessment of Alzheimer-type dementia and individuals affected by some disability that may prevent the subject from completing all study requirements (e.g. language difficulties).

All experiments followed the tenets of the declaration of Helsinki. Both patients and controls gave their informed consent after the aims and the experimental procedures were fully explained. The experimental protocol was previously approved by the local ethical Board of Pisa University Medical School and Neuroscience Department Committee.

2.2. Visual stimuli

Stimuli were designed to preferentially activate functionally separate pathways in the visual system described as magno-cellular (M), parvo-cellular (P) and konio-cellular (K). Visual stimuli were equiluminant horizontal sinusoidal gratings, modulated either in luminance (Y-Bk) and chromaticity (R-G and B-Y). R-G chromatic gratings were obtained by superimposing (out of phase by 180°) red-black to green-black luminance gratings, and blue-yellow chromatic grating were obtained by superimposing (also out of phase by 180°) blue-black to yellow-black luminance gratings. Red-black, green-black, blue-black, and yellow-black luminance gratings had the same Michelson contrast (K) levels (90%), which was used to define the contrast of the chromatic grating. Gratings were generated by a VSG/2 graphic card (Cambridge Research©, UK), displayed full-field on a colour monitor (Samsung Sync Master1100DF®, 21 inches) at a frame rate of 120 Hz and 14 bits per colour per pixel, suitably linearized by gamma correction [59,60].

The equiluminant point was detected for each subject by assessing contrast sensitivity with the method of ascending limits for a 1 c/deg red-green or black-yellow grating [23,60], counterphased at 15 Hz [50]. The point of minimum sensitivity was taken as the equiluminant value for the subject. The relative luminance (r) is easily defined by the usual formula [50]:

$$r = \frac{Lum_{red}}{Lum_{red} + Lum_{green}}$$

where values of $r = 0$, $r = 0.5$ (equiluminant point, at maximum chromatic contrast) and $r = 1.0$ respectively define G-Bk, R-G and R-Bk patterns. Red-green gratings were sinusoidally reversed at 16 Hz and the r-ratio was varied to null or minimize the perception of flicker. The extreme values (i.e. $r = 0$ and $r = 1$) characterize gratings with pure luminance contrast and poor chromatic one [60]. This implies that, at low-spatial frequencies below 5 cycles/deg, contrast sensitivity is greater to the chromatic gratings, consisting of two monochromatic gratings added in anti-phase, than to either monochromatic grating alone. Above 5 cycles/deg, contrast sensitivity is greater to monochromatic than to chromatic gratings. Contrast sensitivity reflects the minimum amount of contrast that an observer needs to resolve a stimulus of a given size.

It is well known that R-G opponent parvocellular cells respond well to chromatic patterns of low-spatial frequencies, whereas magnocellular stream respond only weakly at equiluminance [59,65]: on the other hand, an impairment of Bk-Y grating detection, in terms of VEPs responses of either poor amplitude or latency, is likely related to involvement of magnocellular pathway.

In order to minimize distortions produced by short-wavelength cones activation, each pattern was viewed through yellow filters (Kodak© Wratten 16) that attenuated wavelengths below 500 nm. Mean luminance was kept at 17 cd m^{-2}, inducing a retinal illuminance of 330 Troland when viewed through undilated natural pupils, estimating to be ~3–5 in both patients and normal subjects.

PERGs were recorded monocularly in response to chromatic equiluminant red-green (R-G), blue-yellow (B-Y) and luminance (Lum) yellow-black (Y-Bk) horizontal sinusoidal gratings of 0.3 c/deg and 90% contrast (K), reversed at 1 Hz, displayed on a TV monitor at a viewing distance of 24 cm (59.2 × 59 deg field); PERGs and VEPs were recorded not simultaneously being the stimuli employed chosen to emphasize retinal or cortical responses: we performed firstly ChPERGs and then ChVEPs, consecutively on the same session.

VEPs were recorded in response to full-field (14 deg) chromatic equiluminant R-G, B-Y and luminance Y-Bk sinusoidal gratings of 2 c/deg, presented in onset (300 ms)–offset (700 ms) mode, at a contrast (K) level of 90%.

2.3. Electrophysiological recordings

a. *PERGs*: PERGs have been recorded monocularly using common Ag/AgCl superficial cup electrodes, 9 mm in diameter (electrode impedance < 5 kΩ, inter-electrode one < 500 Ω), the active taped in mid position over the inferior eyelid, the reference on the same position of the contralateral patched eye; the ground was located at the vertex (Cz). PERGs showed a positive–negative waveform (P1–N1) [65,66]; latencies and amplitudes of different waves were measured using the cursor with the digital readout on the monitor: amplitudes from peak to baseline for P1, peak to peak for N1; latencies at P1 and N1 peaks. Sweep duration was 450 ms. Responses to patterns of zero contrast were frequently recorded to have a measure of residual noise.

The use of skin electrodes with an inter-ocular recording represents the better compromise between signal-to-noise ratio and signal stability [56]. Adequate electrical conduction was achieved by cleansing the skin with alcohol and by applying an abrasive cream prior to electrode application.

b. *VEPs*: VEPs were recorded using analogous Ag/AgCl superficial cup electrodes, 9 mm diameter, placed 2 cm above the inion (active) and at the right mastoid (reference); the vertex was grounded. Electrode resistance was kept below 5 kΩ, inter-electrode one less than 500 Ω. VEPs were analyzed in terms of mean amplitude and latency, where the first one corresponded to the voltage difference between the trough and the subsequent peak of the different waves. Normative data for the present set of stimuli and recording conditions have been previously published [60].

2.4. Data post-processing and signal reconstruction

Two traces were obtained for each stimulating pattern to ensure response consistency and then averaged (see Figs. 1 and 2). The subject under examination was seated in a semi-dark, acoustically isolated room in front of the display. Prior to the experiment, each subjects was adapted to the ambient room light for 10 min and were fully corrected according to the different viewing distances of psychophysical and electrophysiological experiments. Signal were amplified (ERG 100,000, VEP 50,000 folds), filtered between 0.3 and 100 Hz (6 dB octave^{-1}), digitised at 1024 Hz with 12 bit resolution and averaged on line by a PC (Olidata®, Cesena, Italy), using a custom software written in Labview language (Version 7.0, National Instruments, Austin, TX, 1998). Sweeps containing signals higher than 4 V, corresponding to final display of 80 μV, were automatically rejected to minimize EEG contamination by eye blinking, ocular movement, or other environmental instrumental-biological activities. Responses were evaluated separately for partial averages (10- or 20-sum packets) of the total average (at least 100 sums) to assess consistency. Further details on recording conditions and normative data used for the present set of stimuli can be found out elsewhere [60].

Responses were evaluated separately for partial averages (PERGs, 100 sum or 10 packets, VEPs 50 sum or 5 packets) of the total average (at least 200 sums) in order to assess consistency and two or three traces for each eye were superimposed to ensure their reproducibility.

Transient PERGs were smoothed off-line by running average over 10 points to cancel most of high-frequency noise coming from eyelid muscle activity, thereby allowing a more precise evaluation of amplitude and latency results.

The subject under examination was seated in a semi-dark, acoustically isolated room in front of the display. All had no or small refractive errors, and were fully corrected according to the different viewing distances of psychophysical and electrophysiological experiments. Subjects were instructed to fixate a black spot at the centre of the video screen and no artificial pupils or dilatory agents were used.

2.5. Statistical analysis

All data were analyzed in terms of peak-amplitude and latency (for both PERG and VEPs) with commercial statistical software (XLSTAT® v. 7.5.2, devised for Windows Excel®, Microsoft Corporation©, 2002). The obtained values were assessed using the Student's *t*-test for paired data. All the results are reported as mean values ± 2SDs.

All studies parameters were evaluated statistically using a ≤0.05 level of significance, except when otherwise specified.

3. Results

3.1. Y-Bk (Lum) grating

Transient exemplificative single waveforms and grand average of PERGs and VEPs, obtained either in controls and AD patients, are summarized in Figs. 1 and 2.

When presented to control subjects (top line), sinusoidal gratings elicited the following PERG response: P1 mean latency 38.1 ± 2.4 ms, a N1 peak mean latency of 73.4 ± 8.6 ms and a mean P1 amplitude, evaluated peak to baseline, of 0.3 ± 0.2 and N1 amplitude (peak to peak) of 1.5 ± 0.90 μV. As regards VEPs, they displayed a characteristic positive–negative–positive complex, with a main N-wave with an average latency of 166.6 ± 6.8 ms and mean amplitude of 3.60 ± 1.20 μV.

In AD patients (bottom line), transient PERGs obtained by Y-Bk pattern, had P1 and N1 peak latency with an average of 61.0 ± 5.2 and 96.1 ± 5.8 ms; a mean amplitude of 0.2 ± 0.3 and 0.36 ± 0.59 μV. The VEPs N-wave showed a mean latency of 188.8 ± 8.6 ms and a mean amplitude of 3.03 ± 0.48 μV (Table 2).

3.2. R-G grating

In control subjects, ChPERG responses consisted mainly of a typical positive–negative (P1–N1) waveform; time to peak of this positive–negative wave and the amplitude of P1 and the following negativity were considered as representatives of latency and amplitude. P1 components exhibited a average latency of 65.5 ± 5.7 ms and a mean amplitude, evaluated peak to baseline, of 0.50 ± 0.3 μV; N1 latency and peak to peak amplitudes values were respectively 126.9 ± 6.8 ms and 1.16 ± 0.93 μV. The colour VEPs displayed a characteristic positive–negative–positive waveform: the main N-wave showed a mean latency of 175.1 ± 6.7 ms, and a mean peak to peak amplitude of 2.1 ± 1.94 μV.

In AD patients, mean latency of R-G P1 and N1 ChPERG components were 62.6 ms ± 7.8 and 131.3 ± 7.8, with a mean amplitude of 0.2 ± 0.14 and 0.47 ± 0.64 μV, respectively. As far as concerns ChVEPs, latency of N-wave was 176.2 ± 11.1 ms, with a mean amplitude of 2.9 ± 1.78 (Table 2).

3.3. B-Y grating

Average latency of P1 and N1 ChPERG components were in controls respectively 65.0 ± 5.6 and 133.3 ± 5.8 ms; they showed a mean amplitude of 0.1 ± 0.3 and 3.31 ± 1.55 μV, respectively. As far as concerns ChVEPs, latency of main N-wave was 180.4 ± 8.8 ms, with mean amplitude of 4.19 ± 1.34 μV.

In AD patients, average latency of P1 and N1 components were respectively 65.0 ± 6.4 ms and 136.3 ± 9.2; they showed a mean amplitude of 0.26 ± 0.6 and 1.30 ± 0.45 μV, respectively. ChVEPs latency of N-wave was 179.1 ± 8.7 ms, with a mean amplitude of 3.71 ± 1.84 μV.

Moreover, statistical analysis revealed that temporal features and mean amplitudes of PERGs as well as VEPs to Y-Bk grating in AD patients differ from those in control subjects ($p \leq 0.01$ and $p \leq 0.05$, respectively). Also amplitude of R-G and B-Y PERGs resulted light reduced in AD patients compared with controls.

In addition, to asses retinal versus post-retinal defects, we evaluated the so-called retino-cortical times (RCT), that is differences between PERG and VEPs, in both groups; we did not found any significant variation between controls and patients in neither of gratings presented (Table 3).

4. Discussion

Our data show evident abnormalities both in latency and amplitude of Lum PERGs in AD patients compared with controls, while no significant differences were found in ChPERGs between the two groups. VEPs and RCT analysis did not revealed a retinocalcarine pathway involvement associated with AD, suggesting the existence of a specific magnocellular or M-pathway deficit.

Previous studies have reported causes an unspecific decline of the response of the visual system to luminance and colour contrast during ageing but failed to provide a strong evidence for a selective deterioration of either parvocellular or magnocellular pathways [23,35]. Since age-dependent modifications were substantially the same for sensitivity to luminance and colour contrast [63,72], it has been argued that they all arise at a peripheral level, with obvious reference to senile miosis [23], increased intraocular light scatter, decreased retinal blood flow in narrow veins [5] or opacification of the ocular media [76], promoted by regionally specific Aβ proteins aggregation. Some authors have also described a disease-related enlargement of the optic nerve head cupping as well as a marked thinning of neuroretinal rim [5]. Others raised the hypothesis that retinal ganglion cell loss, likely as a consequence of retrograde axonal degeneration, might also be involved in visual deficits reported in AD [4,53]. However, a combination of these mechanisms is also conceivable [53].

Another important issue is whether loss of retinal ganglion cells is due to disease-related amyloidosis or to a primary optic neuropathy [3,35]. More recently, this viewpoint has being challenged and many studies provides strong evidences that spontaneous generation of colour is at least partly mediated by the rebound inhibition of adapted wavelength selective cells in V1 [11,18]. The existence of a wide range of visual variants of AD, characterized by

different clinical presentation at onset, has been progressively recognized [1,11,31,57]. For instance, Pietrini et al. [57], using in vivo measures of brain metabolism, described a distinctive AD patients subgroup characterized by visual symptoms, without any lack in glucose metabolism within frontal lobe regions, thus with fully preserved memory. These increasing findings lead us to accurately explore specific visual impairments in AD. Evidence beyond the retina linked to poor transmission of visual information through retinocalcarine pathway is not proved by present results as RCT was within normal limits.

Surprisingly, in previous studies individuals who were too confused to perform simple psychometric tests were able to cooperate enough to have pattern reversal visual evoked potentials recordings [88,89]. Thus, despite the lack of significant difference between AD and depressed patients, some authors [39,46] were able to differentiate the two conditions.

The neural activity in the M-pathway is the best candidate to be the high contrast mechanism detected with pattern reversal and pattern onset/offset VEPs [69]. AD causes a wide and multi-focal neuronal degeneration affecting visual areas within occipital, temporal and parietal cortex [62]. Another weighting variable is the non-linear characteristics of the response generators [59]: most of the magnocellular elements could mainly contribute to the second harmonic of the PERGs and VEPs, especially when Bk-Y grating is presented.

The involvement of magnocellular stream in AD could be demonstrated by both retinal and cortico-subcortical evidences. By the way, Sadun et al. [64] observed that while the P-stream is relatively spared, the largest retinal cells seemed to be selectively affected by neural degeneration and argued that M-pathway may be involved in some cases of AD. Few years later, Parisi et al. [56] reported that there was a significant correlation between the thinning of the neural fiber layer and the ERG responses. On the other hand, Hof et al. [32], studying AD patients with prominent visual deficits, described a high concentration of neurofibrillary tangles in area V5 as compared to their occipital fields, likely due to an extensive M-pathway impairment.

Our findings are consistent with a sparing of foveal retino-cortical pathways and with the selective impairment of either corticocortical connections between the striate cortex and the visual associative structures or the temporo-parieto-occipital visual areas, indicating the different vulnerability of specific pathways during AD progression. In addition our results are in agreement with Trick et al. [81], that found a significant reduction in the amplitude of ERG responses possibly driven by the magno-cellular stream of visual processing. From a cellular point of view, the dorsal visual pathway, commonly named “where” pathway, is composed mainly of cells of the magnocellular system, whereas the ventral one, defined as “what” pathway, contains both magnocellular and parvocellular cells [51], even though histological and in vivo evidences in our species are still lacking. Di Russo and Spinelli [18] suggested a major involvement of the magnocellular stream in high-order visual processing, addressing this hypothesis by comparing effects of spatial attention on VEPs recording for luminance (yellow-black) and chromatic (red-green) stimuli.

Thus, our findings suggest a deficit in primary visual processing and a selective deficit in secondary visual processing in moderate cases of dementia [9]. The shift is most prominent for black-yellow gratings. Unfortunately, partial-field stimulation, characterized by an increased diagnostic yield, did not perform in our study and requires a modified method.

In our relatively small samples, statistical analysis of retino-cortical conduction times, as well as analysis of P1-wave’s latency and amplitude, did not show any significant difference between control group and patients: although not yet completely proven, this suggests that M-stream activation primarily involves extra-geniculate pathways, as firstly reported by Moore [49] and later described by Jacob et al. [33]. Others [9] reporting P1 differences,

suggest the possibility of the activation of a particular cluster of magnocellular cells more sensitive to poor chromatic contrasts and probably related to a selective deficit in secondary visual processing in moderate cases of dementia. Thus representing a less reliable electrophysiological marker in AD.

It is worth pointing out that P1 may be prolonged, but more commonly its amplitude is decreased disproportionately to the change in latency [27,42] and difficult to correlate with specific lesions occurred within visual central pathways. These differential injuries highlight novel insights into the pathology of AD; taken together, we provide here a compelling evidence for the existence of a selective deficit of magnocellular system in AD. However, the possibility of a selective parvocellular impairment or a widespread visual deficit cannot be easily ruled out.

For instance, it cannot be excluded that the outer retina may show some signs of impairment in AD patients: in fact, age-dependent morphological alterations in second-order retinal neurons is commonly accompanied by dendrites loss, redistribution of glutamate receptors and simplification of horizontal cells network [71,74]. Blanks and colleagues found that largest ganglion cells may have been preferentially affected in AD [6,7]. These all processes are characterized by a clear spatial gradient, increasing in number from the centre to the periphery of the retina [24,36]. Some authors concluded that the unspecific alterations in second-order neurons pool reflects an initial age-dependent photoreceptors dysfunctions [28]. However, it is worth remembering that compensatory remodeling, in relation to gradual increase in both ectopic synapses and collateral sprouting, follows a similar trend [74]: it is likely that retinal ganglion cell loss may be partially secondary to retrograde axonal degeneration [29].

We believe that further studies should be conducted with larger sample sizes to confirm these results and expanded to include other forms of vision testing; it is desirable that better understanding of vision-related impairment could guide interventions to improve functional capacity in patients with dementia.

Acknowledgments

We wish to thank all the neurologists of Neuroscience Department, Unit of Neurology, at Pisa University Medical School, who referred their patients and permitted us to examine them. We gratefully acknowledge the participation of all subjects, as well as Mr. P. Orsini for his excellent technical assistance.

Acknowledgment is made to the donors of the Alzheimer's Disease Research, a program of American Health Assistance Foundation (AHAF grant, A2008-335).

The paper was supported in part by the Italian operating and development MIUR PRIN grant year 2006, n. 2006062332 002.

References

1. Albert MS, Duffy FH, McAnulty GB. Electrophysiologic comparisons between two groups of patients with Alzheimer's disease. Arch Neurol. 1990; 47:857–863. [PubMed: 2375691]
2. Aoki C, Kabak S. Cholinergic terminals in the cat visual cortex: ultrastructural basis for interaction with glutamate-immunoreactive neurons and other cells. Vis Neurosci. 1992; 8:177–191. [PubMed: 1347700]
3. Bayer AU, Ferrari F, Erb C. High occurrence rate of glaucoma among patients with Alzheimer's disease. Eur Neurol. 2002; 47:165–168. [PubMed: 11914555]
4. Beelke M, Sannita WG. Cholinergic function and dysfunction in the visual system. Methods Find Exp Clin Pharmacol. 2002; 24(Suppl D):113–117. [PubMed: 12575477]

5. Berisha F, Feke GT, Trempe CL, McMeel JW, Schepens CL. Retinal abnormalities in early Alzheimer's disease. Invest Ophthalmol Vis Sci. 2007; 48:2285–2289. [PubMed: 17460292]
6. Blanks JC, Hinton DR, Sadun AA, Miller CA. Retinal ganglion cell degeneration in Alzheimer's disease. Brain Res. 1989; 501:364–372. [PubMed: 2819446]
7. Blanks JC, Schmidt SY, Torigoe Y, Porrello KV, Hinton DR, Blanks RH. Retinal pathology in Alzheimer's disease. II. Regional neuron loss and glial changes in GCL. Neurobiol Aging. 1996; 17:385–395. [PubMed: 8725900]
8. Boxer AL, Kramer JH, Du AT, Schuff N, Weiner MW, Miller BL, Rosen HJ. Focal right inferotemporal atrophy in AD with disproportionate visual constructive impairment. Neurology. 2003; 61:1485–1491. [PubMed: 14663029]
9. Brodie EE, Allan D, Brooks DN, McCulloch J, Foulds WS. Flash and pattern reversal visual evoked responses in normal and demented elderly. Cortex. 1992; 28:289–293. [PubMed: 1499313]
10. Campbell FW, Green DG. Optical and retinal factors affecting visual resolution. J Physiol. 1965; 181:576–593. [PubMed: 5880378]
11. Coburn KL, Ashford JW, Moreno MA. Visual evoked potentials in dementia: selective delay of flash P2 in probable Alzheimer's disease. J Neuropsych Clin Neurosci. 1991; 3:431–435.
12. Cormack FK, Tovee M, Ballard C. Contrast sensitivity and visual acuity in patients with Alzheimer's disease. Int J Geriatr Psych. 2000; 15:614–620.
13. Cronin-Golomb A, Rizzo JF, Corkin S, Growdon JH. Visual function in Alzheimer's disease and normal aging. Ann N Y Acad Sci. 1991; 640:28–35. [PubMed: 1776752]
14. Crow RW, Levin LB, LaBree L, Rubin R, Feldon SE. Sweep visual evoked potential evaluation of contrast sensitivity in Alzheimer's dementia. Invest Ophthalmol Vis Sci. 2003; 44:875–878. [PubMed: 12556424]
15. Crum RM, Anthony JC, Bassett SS, Folstein MF. Population-based norms for the Mini-Mental State Examination by age and educational level. JAMA. 1993; 269:2386–2391. [PubMed: 8479064]
16. Dacey DM, Lee BB. The 'blue-on' opponent pathway in primate retina originates from a distinct bistratified ganglion cell type. Nature. 1994; 367:731–735. [PubMed: 8107868]
17. De Monasterio FM, Gouras P. Functional properties of ganglion cells of the rhesus monkey retina. J Physiol. 1975; 251:167–195. [PubMed: 810576]
18. Di Russo F, Spinelli D. Spatial attention has different effects on the magno- and parvocellular pathways. NeuroReport. 1999; 10:2755–2762. [PubMed: 10511435]
19. Drachman DA, Lippa CF. The etiology of Alzheimer's disease: the pathogenesis of dementia. The role of neurotoxins. Ann N Y Acad Sci. 1992; 648:176–186. [PubMed: 1637045]
20. Dreher B, Fukada Y, Rodieck RW. Identification, classification and anatomical segregation of cells with X-like and Y-like properties in the lateral geniculate nucleus of old-world primates. J Physiol. 1976; 258:433–452. [PubMed: 822151]
21. Engel S, Zhang X, Wandell B. Colour tuning in human visual cortex measured with functional magnetic resonance imaging. Nature. 1997; 388:68–71. [PubMed: 9214503]
22. Erkinjuntti T, Ketonen L, Sulkava R, Sipponen J, Vuorialho M, Iivanainen M. Do white matter changes on MRI and CT differentiate vascular dementia from Alzheimer's disease? J Neurol Neurosurg Psychiatry. 1987; 50:37–42. [PubMed: 3819754]
23. Fiorentini A, Porciatti V, Morrone MC, Burr DC. Visual ageing: unspecific decline of the responses to luminance and colour. Vision Res. 1996; 36:3356–3557.
24. Fisher RF. The variations of the peripheral visual fields with age. Doc Ophthalmol. 1968; 24:41–67. [PubMed: 5681957]
25. Giannakopoulos P, Gold G, Duc M, Michel JP, Hof PR, Bouras C. Neuroanatomic correlates of visual agnosia in Alzheimer's disease: a clinico-pathologic study. Neurology. 1999; 52:71–77. [PubMed: 9921851]
26. Grant WB, Campbell A, Itzhaki RF, Savory J. The significance of environmental factors in the etiology of Alzheimer's disease. J Alzheimers Dis. 2002; 4:179–189. [PubMed: 12226537]
27. Grayson AS, Weiler EM, Sandman DE. Visual evoked potentials in early Alzheimer's dementia: an exploratory study. J Gen Psychol. 1995; 122:113–129. [PubMed: 7714499]

28. Gresh J, Goletz PW, Crouch RK, Rohrer B. Structure–function analysis of rods and cones in juvenile, adult, and aged C57bl/6 and Balb/c mice. Vis Neurosci. 2003; 20:211–220. [PubMed: 12916741]
29. Hinton DR, Sadun AA, Blanks JC, Miller CA. Optic-nerve degeneration in Alzheimer's disease. N Engl J Med. 1986; 315:485–487. [PubMed: 3736630]
30. Hof PR, Bierer LM, Perl DP, Delacourte A, Buee L, Bouras C, Morrison JH. Evidence for early vulnerability of the medial and inferior aspects of the temporal lobe in an 82-year-old patient with preclinical signs of dementia. Regional and laminar distribution of neurofibrillary tangles and senile plaques. Arch Neurol. 1992; 49:946–953. [PubMed: 1520086]
31. Hof PR, Morrison JH. Quantitative analysis of a vulnerable subset of pyramidal neurons in Alzheimer's disease: II. Primary and secondary visual cortex. J Comp Neurol. 1990; 301:55–64. [PubMed: 1706358]
32. Hof PR, Vogt BA, Bouras C, Morrison JH. Atypical form of Alzheimer's disease with prominent posterior cortical atrophy: a review of lesion distribution and circuit disconnection in cortical visual pathways. Vision Res. 1997; 37:3609–3625. [PubMed: 9425534]
33. Jacob B, Hache JC, Pasquier F. Dysfunction of the magnocellular pathway in Alzheimer's disease. Rev Neurol (Paris). 2002; 158:555–564. [PubMed: 12072823]
34. Johnson KA, Davis KR, Buonanno FS, Brady TJ, Rosen TJ, Growdon JH. Comparison of magnetic resonance and roentgen ray computed tomography in dementia. Arch Neurol. 1987; 44:1075–1080. [PubMed: 3632382]
35. Kergoat H, Kergoat MJ, Justino L, Chertkow H, Robillard A, Bergman H. Visual retinocortical function in dementia of the Alzheimer type. Gerontology. 2002; 48:197–203. [PubMed: 12053107]
36. Lai YL, Jacoby RO, Jonas AM. Age-related and light-associated retinal changes in Fischer rats. Invest Ophthalmol Vis Sci. 1978; 17:634–638. [PubMed: 669893]
37. Lakshminarayanan V, Lagrave J, Kean ML, Dick M, Shankle R. Vision in dementia: contrast effects. Neurol Res. 1996; 18:9–15. [PubMed: 8714529]
38. Lennie P, Krauskopf J, Sclar G. Chromatic mechanisms in striate cortex of macaque. J Neurosci. 1990; 10:649–669. [PubMed: 2303866]
39. Levy JA, Chelune GJ. Cognitive-behavioral profiles of neurodegenerative dementias: beyond Alzheimer's disease. J Geriatr Psychiatry Neurol. 2007; 20:227–238. [PubMed: 18004009]
40. Liang WS, Dunckley T, Beach TG, Grover A, Mastroeni D, Ramsey K, Caselli RJ, Kukull WA, McKeel D, Morris JC, Hulette CM, Schmechel D, Reiman EM, Rogers J, Stephan DA. Altered neuronal gene expression in brain regions differentially affected by Alzheimer's disease: a reference data set. Physiol Genom. 2008; 33:240–256.
41. Livingstone MS, Hubel DH. Do the relative mapping densities of the magno-and parvocellular systems vary with eccentricity? J Neurosci. 1988; 8:4334–4339. [PubMed: 3183725]
42. Martinelli V, Locatelli T, Comi G, Lia C, Alberoni M, Bressi S, Rovaris M, Franceschi M, Canal N. Pattern visual evoked potential mapping in Alzheimer's disease: correlations with visuospatial impairment. Dementia. 1996; 7:63–68. [PubMed: 8866677]
43. Maunsell JH, Newsome WT. Visual processing in monkey extrastriate cortex. Annu Rev Neurosci. 1987; 10:363–401. [PubMed: 3105414]
44. McKhann G, Drachman D, Folstein M, Katzman R, Price D, Stadlan EM. Clinical diagnosis of Alzheimer's disease: report of the NINCDS-ADRDA Work Group under the auspices of Department of Health and Human Services Task Force on Alzheimer's Disease. Neurology. 1984; 34:939–944. [PubMed: 6610841]
45. Mendez MF, Ghajarania M, Perryman KM. Posterior cortical atrophy: clinical characteristics and differences compared to Alzheimer's disease. Dement Geriatr Cogn Disord. 2002; 14:33–40. [PubMed: 12053130]
46. Mendez MF, Tomsak RL, Remler B. Disorders of the visual system in Alzheimer's disease. J Clin Neuroophthalmol. 1990; 10:62–69. [PubMed: 2139054]
47. Merigan WH. Chromatic and achromatic vision of macaques: role of the P pathway. J Neurosci. 1989; 9:776–783. [PubMed: 2926482]

48. Merigan WH, Maunsell JH. How parallel are the primate visual pathways? Annu Rev Neurosci. 1993; 16:369–402. [PubMed: 8460898]
49. Moore NC. Visual evoked responses in Alzheimer's disease: a review. Clin Electroencephalogr. 1997; 28:137–142. [PubMed: 9241466]
50. Mullen KT. The contrast sensitivity of human colour vision to red-green and blue-yellow chromatic gratings. J Physiol. 1985; 359:381–400. [PubMed: 3999044]
51. Nealey TA, Maunsell JH. Magnocellular and parvocellular contributions to the responses of neurons in macaque striate cortex. J Neurosci. 1994; 14:2069–2079. [PubMed: 8158257]
52. Ng S, Villemagne VL, Berlangieri S, Lee ST, Cherk M, Gong SJ, Ackermann U, Saunder T, Tochon-Danguy H, Jones G, Smith C, O'Keefe G, Masters CL, Rowe CC. Visual assessment versus quantitative assessment of 11C-PIB PET and 18F-FDG PET for detection of Alzheimer's disease. J Nucl Med. 2007; 48:547–552. [PubMed: 17401090]
53. Nobili L, Sannita WG. Cholinergic modulation, visual function and Alzheimer's dementia. Vision Res. 1997; 37:3559–3571. [PubMed: 9425531]
54. Onofrj M, Gambi D, Del Re ML, Fulgente T, Bazzano S, Colamartino P, Malatesta G. Mapping of event-related potentials to auditory and visual odd-ball paradigms in patients affected by different forms of dementia. Eur Neurol. 1991; 31:259–269. [PubMed: 1868869]
55. Origlia N, Capsoni S, Cattaneo A, Fang F, Arancio O, Yan SD, Domenici L. A beta-dependent inhibition of LTP in different intracortical circuits of the visual cortex: the role of RAGE. J Alzheimers Dis. 2009; 17:59–68. [PubMed: 19221410]
56. Parisi V, Restuccia R, Fattapposta F, Mina C, Bucci MG, Pierelli F. Morphological and functional retinal impairment in Alzheimer's disease patients. Clin Neurophysiol. 2001; 112:1860–1867. [PubMed: 11595144]
57. Pietrini P, Furey ML, Graff-Radford N, Freo U, Alexander GE, Grady CL, Dani A, Mentis MJ, Schapiro MB. Preferential metabolic involvement of visual cortical areas in a subtype of Alzheimer's disease: clinical implications. Am J Psychiatry. 1996; 153:1261–1268. [PubMed: 8831432]
58. Pollock VE, Schneider LS, Chui HC, Henderson V, Zemansky M, Sloane RB. Visual evoked potentials in dementia: a meta-analysis and empirical study of Alzheimer's disease patients. Biol Psychiatry. 1989; 25:1003–1013. [PubMed: 2720014]
59. Porciatti V, Sartucci F. Retinal and cortical evoked responses to chromatic contrast stimuli. Specific losses in both eyes of patients with multiple sclerosis and unilateral optic neuritis. Brain. 1996; 119(Pt3):723–740. [PubMed: 8673486]
60. Porciatti V, Sartucci F. Normative data for onset VEPs to red-green and blue-yellow chromatic contrast. Clin Neurophysiol. 1999; 110:772–781. [PubMed: 10378751]
61. Rizzo JF III, Cronin-Golomb A, Growdon JH, Corkin S, Rosen TJ, Sand-berg MA, Chiappa KH, Lessell S. Retinocalcarine function in Alzheimer's disease. A clinical and electrophysiological study. Arch Neurol. 1992; 49:93–101. [PubMed: 1728270]
62. Rizzo M, Anderson SW, Dawson J, Nawrot M. Vision and cognition in Alzheimer's disease. Neuropsychologia. 2000; 38:1157–1169. [PubMed: 10838150]
63. Ruddock K. The effect of age upon colour vision. II. Changes with age in light transmission of the ocular media. Vision Res. 1965; 5:47–58. [PubMed: 5862761]
64. Sadun AA, Borchert M, DeVita E, Hinton DR, Bassi CJ. Assessment of visual impairment in patients with Alzheimer's disease. Am J Ophthalmol. 1987; 104:113–120. [PubMed: 3618708]
65. Sartucci F, Orlandi G, Bonuccelli U, Borghetti D, Murri L, Orsini C, Domenici L, Porciatti V. Chromatic pattern-reversal electroretinograms (ChPERGs) are spared in multiple system atrophy compared with Parkinson's disease. Neurol Sci. 2006; 26:395–401. [PubMed: 16601931]
66. Sartucci F, Orlandi G, Lucetti C, Bonuccelli U, Murri L, Orsini C, Porciatti V. Changes in pattern electroretinograms to equiluminant red-green and blue-yellow gratings in patients with early Parkinson's disease. J Clin Neurophysiol. 2003; 20:375–381. [PubMed: 14701999]
67. Sartucci F, Porciatti V. Visual-evoked potentials to onset of chromatic red-green and blue-yellow gratings in Parkinson's disease never treated with L-dopa. J Clin Neurophysiol. 2006; 23:431–435. [PubMed: 17016154]

68. Shapley R. Visual sensitivity and parallel retinocortical channels. Annu Rev Psychol. 1990; 41:635–658. [PubMed: 2407178]
69. Souza GS, Gomes BD, Lacerda EM, Saito CA, da Silva Filho M, Silveira LC. Amplitude of the transient visual evoked potential (tVEP) as a function of achromatic and chromatic contrast: contribution of different visual pathways. Vis Neurosci. 2008; 25:317–325. [PubMed: 18321403]
70. Spear P. Neural bases of visual deficits during aging. Vision Res. 1993; 33:2589–2609. [PubMed: 8296455]
71. Strettoi E, Porciatti V, Falsini B, Pignatelli V, Rossi C. Morphological and functional abnormalities in the inner retina of the rd/rd mouse. J Neurosci. 2002; 22:5492–5504. [PubMed: 12097501]
72. Suzuki TA, Qiang Y, Sakuragawa S, Tamura H, Okajima K. Age-related changes of reaction time and p300 for low-contrast color stimuli: effects of yellowing of the aging human lens. J Physiol Anthropol. 2006; 25:179–187. [PubMed: 16679715]
73. Tanaka F, Kachi T, Yamada T, Sobue G. Auditory and visual event-related potentials and flash visual evoked potentials in Alzheimer's disease: correlations with Mini-Mental State Examination and Raven's Coloured Progressive Matrices. J Neurol Sci. 1998; 156:83–88. [PubMed: 9559992]
74. Terzibasi E, Calamusa M, Novelli E, Domenici L, Strettoi E, Cellerino A. Age-dependent remodelling of retinal circuitry. Neurobiol Aging. 2009; 30:819–828. [PubMed: 17920161]
75. Tierney MC, Fisher RH, Lewis AJ, Zorzitto ML, Snow WG, Reid DW, Nieuwstraten P. The NINCDS-ADRDA Work Group criteria for the clinical diagnosis of probable Alzheimer's disease: a clinicopathologic study of 57 cases. Neurology. 1988; 38:359–364. [PubMed: 3347338]
76. Tobimatsu S. Aging and pattern visual evoked potentials. Optom Vis Sci. 1995; 72:192–197. [PubMed: 7609942]
77. Tobimatsu S, Hamada T, Okayama M, Fukui R, Kato M. Temporal frequency deficit in patients with senile dementia of the Alzheimer type: a visual evoked potential study. Neurology. 1994; 44:1260–1263. [PubMed: 8035926]
78. Tognoni G, Ceravolo R, Nucciarone B, Bianchi F, Dell'Agnello G, Ghicopulos I, Siciliano G, Murri L. From mild cognitive impairment to dementia: a prevalence study in a district of Tuscany, Italy. Acta Neurol Scand. 2005; 112:65–71. [PubMed: 16008529]
79. Tootell RB, Hamilton SL, Switkes E. Functional anatomy of macaque striate cortex. IV. Contrast and magno–parvo streams. J Neurosci. 1988; 8:1594–1609. [PubMed: 3367212]
80. Tootell RB, Switkes E, Silverman MS, Hamilton SL. Functional anatomy of macaque striate cortex. II. Retinotopic organization. J Neurosci. 1988; 8:1531–1568. [PubMed: 3367210]
81. Trick GL, Trick LR, Morris P, Wolf M. Visual field loss in senile dementia of the Alzheimer's type. Neurology. 1995; 45:68–74. [PubMed: 7824139]
82. Van Essen DC, Gallant JL. Neural mechanisms of form and motion processing in the primate visual system. Neuron. 1994; 13:1–10. [PubMed: 8043270]
83. Victor JD, Purpura KP, Conte MM. Chromatic and luminance interactions in spatial contrast signals. Vis Neurosci. 1998; 15:607–624. [PubMed: 9682865]
84. Visser SL, Stam FC, van Tilburg W, den Velde W, Blom JL, de Rijke W. Visual evoked response in senile and presenile dementia. Electroencephalogr Clin Neurophysiol. 1976; 40:385–392. [PubMed: 56264]
85. Visser SL, Van Tilburg W, Hooijer C, Jonker C, De Rijke W. Visual evoked potentials (VEPs) in senile dementia (Alzheimer type) and in non-organic behavioural disorders in the elderly; comparison with EEG parameters. Electroencephalogr Clin Neurophysiol. 1985; 60:115–121. [PubMed: 2578362]
86. Waldemar G, Dubois B, Emre M, Georges J, McKeith IG, Rossor M, Scheltens P, Tariska P, Winblad B. Recommendations for the diagnosis and management of Alzheimer's disease and other disorders associated with dementia: EFNS guideline. Eur J Neurol. 2007; 14:e1–e26. [PubMed: 17222085]
87. Whitehouse PJ. Understanding the etiology of Alzheimer's disease. Current approaches. Neurol Clin. 1986; 4:427–437. [PubMed: 2940457]
88. Wright CE, Harding GF, Orwin A. The flash and pattern VEP as a diagnostic indicator of dementia. Doc Ophthalmol. 1986; 62:89–96. [PubMed: 3956362]

89. Wright GM, Richardson CE. Serial visual evoked potential recordings in Alzheimer's disease. Br Med J (Clin Res Ed). 1986; 293:564–565.

90. Young IR, Randell CP, Kaplan PW, James A, Bydder GM, Steiner RE. Nuclear magnetic resonance (NMR) imaging in white matter disease of the brain using spin–echo sequences. J Comput Assist Tomogr. 1983; 7:290–294. [PubMed: 6833562]

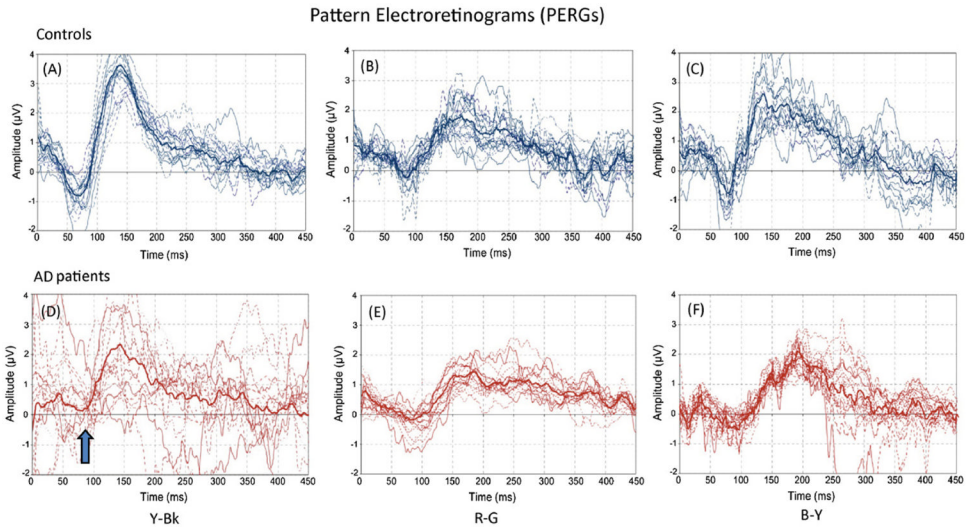

Fig. 1.

Transient PERGs in response to either Y-Bk luminance grating (A and D), equiluminant chromatic R-G (B and E) and B-Y (C and F) in controls (top traces) and AD patients (bottom traces). For each inset, individual waveform are represented by dotted line, the grand mean by bold line. Note the amplitude loss for Y-Bk stimuli (A and D) and B-Y (C and F) stimuli.

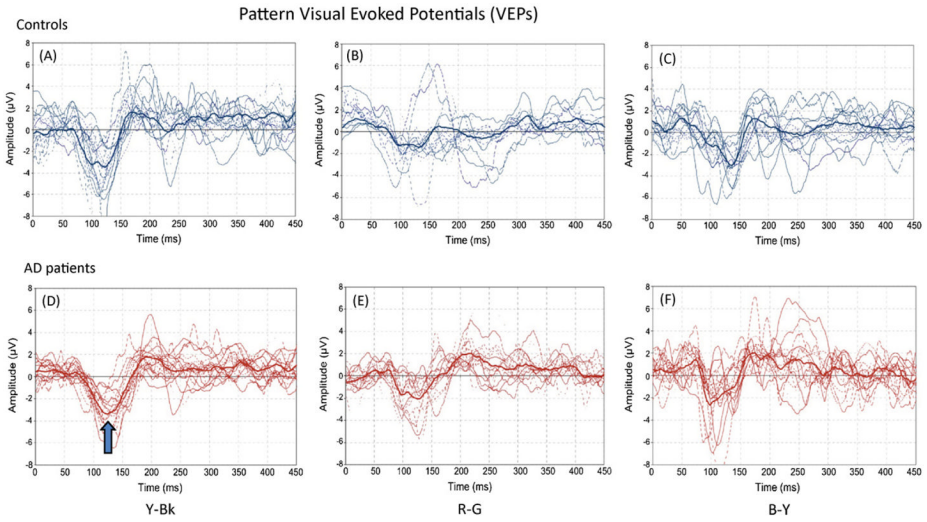

Fig. 2.

Transient VEPs in response to either Y-Bk luminance grating (A and D), R-G (B and E) and B-Y (C and F) in controls (top traces) and AD patients (bottom traces). As in previous figure, for each inset, individual waveform are represented by dotted line, the grand mean by bold line. Note the latency delay for Y-Bk and B-Y stimuli, whereas R-G are relatively spared.

Table 1

Criteria followed to diagnose patients before enrollment in the study.

Exam	Diagnostic features	Key references
Physical findings[a]	Age > 40 years	McKhann et al. [44] Tierney et al. [75]
MMSE[a]	$\leq 23/30$	McKhann et al. [44] Tierney et al. [75]
Neuroimaging (CT scan and/or MRI)	Cortical thinning; severe hippocampal sclerosis; periventricular leukoaraiosis; normotensive hydrocephalus	Erkinjuntti et al. [22]
EEG	Marked slowing of dominant rhythm; persistence of δ- and θ-waves	Albert et al. [1]

[a] NINCDS and ADRDA criteria [86].

Table 2

latency and amplitude of Lum (Bk-Y) and Ch (R-G, B-Y) PERG and PEV, both in controls (Cts) and AD patients ± 1SD.

	PERG						VEPs		
	Y-Bk P1 (±2 Δ*S*)	**Y-Bk N1 (±2 Δ*S*)**	**R-G P1 (±2 Δ*S*)**	**R-G N1 (±2 Δ*S*)**	**B-Y P1 (±2 Δ*S*)**	**B-Y N1 (±2 Δ*S*)**	**Y-Bk N-wave (±2 Δ*S*)**	**R-G N-wave (±2 Δ*S*)**	**B-Y N-wave (±2 Δ*S*)**
Cts-latency (ms)	38.1 ± 2.4	73.4 ± 8.6	65.5 ± 5.7	126.9 ± 6.8	65.0 ± 5.6	133.3 ± 5.8	166.6 ± 6.8	175.1 ± 6.7	180.4 ± 8.8
AD-latency (ms)	61.0 ± 5.2**	96.1 ± 5.8*	62.6 ± 7.8	131.3 ± 7.8	65.0 ± 6.4	136.3 ± 9.2	188.8 ± 8.6*	176.2 ± 11.1	179.1 ± 8.7
Cts-amplitude (μV)	0.3 ± 0.2	1.5 ± 0.90	0.50 ± 0.3	1.16 ± 0.93	0.1 ± 0.3	3.31 ± 1.55	3.60 ± 1.20	2.1 ± 1.94	4.19 ± 1.34
AD-amplitude (μV)	0.2 ± 0.3*	0.36 ± 0.59*	0.2 ± 0.14*	0.47 ± 0.64	0.26 ± 0.6	1.30 ± 0.45*	3.03 ± 0.48*	2.9 ± 1.78	3.71 ± 1.84

* $p \leq 0.05$.

** $p \leq 0.01$.

Table 3

Retino-cortical times for Lum (Bk-Y) and Ch (R-G, B-Y) stimuli, both in controls (Cts) and AD patients ± 1SD.

	Y-Bk	R-G	B-Y
Cts	93.2 ± 7.8	48.2 ± 6.8	47.1 ± 7.3
AD	92.7 ± 7.4	44.9 ± 8.7	42.8 ± 7.9